HHS Public Access

Author manuscript

Science. Author manuscript; available in PMC 2023 April 11.

Published in final edited form as:

Science. 2022 September 23; 377(6613): eabl3921. doi:10.1126/science.abl3921.

Pitx2 patterns an accelerator-brake mechanical feedback through latent TGFβ to rotate the gut

Bhargav D. Sanketi[1], **Noam Zuela-Sopilniak**[2], **Elizabeth Bundschuh**[1], **Sharada Gopal**[1], **Shing Hu**[1], **Joseph Long**[2], **Jan Lammerding**[2], **Sevan Hopyan**[3,4], **Natasza A. Kurpios**[1,*]

[1]Department of Molecular Medicine, College of Veterinary Medicine, Cornell University, Ithaca, NY 14853, USA.

[2]Weill Institute for Cell and Molecular Biology and Department of Biomedical Engineering, Cornell University, Ithaca, NY 14850, USA.

[3]Program in Developmental and Stem Cell Biology, Research Institute, The Hospital for Sick Children, Toronto, Ontario M5G 0A4, Canada.

[4]Department of Molecular Genetics, University of Toronto, Toronto, Ontario M5S 1A8, Canada.

Graphical Abstract

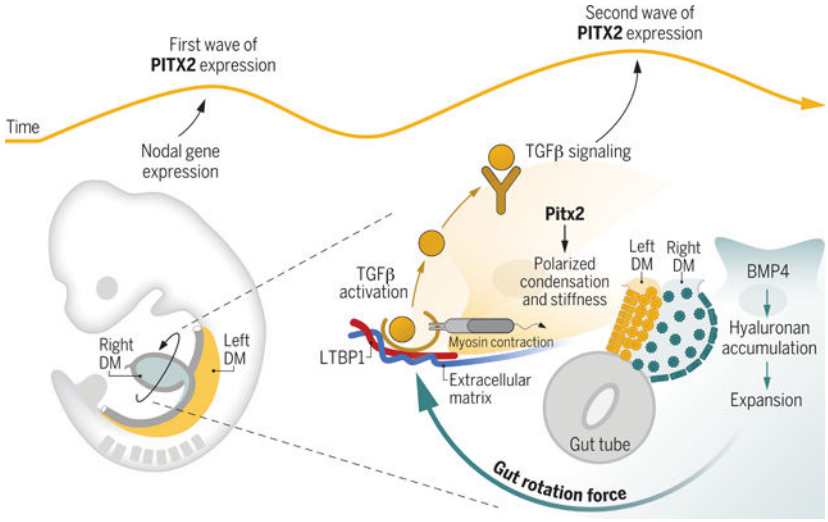

Gut rotation requires a second wave of *Pitx2* expression tuned by the latent TGFβ mechanosensor.

The second *Pitx2* wave represses BMP4 on the left, but BMP4 persists on the right side to drive tissue expansion, initiating gut rotation. Tilting forces from expansion (accelerator) deform the ECM-resident Ltbp1, liberating TGFβ from the latent complex to initiate its downstream

*Corresponding author. natasza.kurpios@cornell.edu.

Author contributions:

Conceptualization: B.D.S., N.A.K.; Funding acquisition: N.A.K.; Investigation: B.D.S.; Methodology: B.D.S., E.B., S.G., S.H., J.L., N.Z.S., J.L.; Supervision: N.A.K.; Visualization: B.D.S., E.B.; Writing: B.D.S., N.A.K.

Data and materials availability: All data are available in the main text or the supplementary materials.

Competing interests: The authors declare no competing interests.

signaling. TGFβ-dependent *Pitx2* expression then causes polarized condensation and increased tissue stiffness (brake), a mechanical feedback loop with the right side.

Research Article Summary

INTRODUCTION: Nearly all vertebrate animals appear symmetrical on the outside, but internal organs such as the heart, liver, and stomach are carefully arranged in a left-right asymmetric pattern. This packs the organs into the limited space of the body while preserving their function. An important model to study left-right organ asymmetry is the process of gut rotation, during which the intestine achieves its familiar twisted form. Gut rotation is predictable in healthy embryos: always counter-clockwise and timed perfectly. Gut rotation hinges on the neighboring dorsal mesentery (DM), a mesodermal tissue bridge anchoring the gut tube through which intestinal blood and lymphatic vessels traverse. The left and right sides of the DM are physically continuous but exhibit discrete and asymmetric tissue changes, causing the mesentery to deform and tilt the attached gut tube leftward. This leftward tilt provides a critical bias to initiate asymmetric gut rotation that is conserved throughout evolution. Gut rotation is orchestrated by the transcription factor *Pitx2*, which is expressed on the left side of embryos. *Pitx2*-driven asymmetry is also evolutionarily conserved, and altered *Pitx2* activity disrupts the growth of lateralized organs.

RATIONALE: In early embryos, *Pitx2* expression is induced during gastrulation by the highly conserved morphogen *Nodal*, a member of the transforming growth factor-β (TGFβ) super-family. This asymmetric *Nodal* expression is transient and stops before asymmetric organ morphogenesis. However, *Pitx2* expression is present on the left side in most asymmetric organs, including the DM, where it orchestrates gut rotation. This has left unresolved the question of how *Pitx2* directs organ development when Nodal is gone. We reasoned that *Pix2* expression during gut rotation must be locally regulated by undescribed mechanisms that are required to correctly shape asymmetric organs.

RESULTS: We found that deletion of Nodal from the mouse lateral plate mesoderm, a precursor of the DM, preserved normal gut laterality and *Pitx2* expression, supporting the presence of additional mechanisms regulating *Pitx2*. Indeed, *Pitx2* expression in the left DM was not continuous and required a second wave of induction during gut rotation. This second wave of *Pitx2* expression was tuned by a local positive feedback loop through the latent TGFβ mechanosensor, a new player here that links *Pitx2* expression to the mechanical forces driving rotation. TGFβ-Pitx2 activity repressed bone morphogenetic protein 4 (*Bmp4*) expression in the left mesentery, marking the first molecular asymmetry of gut rotation. BMP4 signaling persisted to drive the right-side program, which acted through the extracellular matrix (ECM) component hyaluronan to expand and deform the right side of the mesentery, initiating gut rotation. Tilting forces from this right-sided expansion were then sensed and mechanically transduced into TGFβ-dependent *Pitx2* expression changes in the neighboring left DM, resulting in polarized mesenchymal condensation and increased tissue stiffness. These findings can be explained by an accelerator on the right (BMP4) and a brake on the left (TGFβ-*Pitx2*), which cooperate through mechanical feedback to tune the conserved counterclockwise gut rotation. Thus, vertebrate gut rotation combines biochemical and biomechanical inputs to break gut symmetry and direct the evolutionarily conserved intestinal rotation.

CONCLUSION: We uncovered a mechanosensitive TGFβ feedback loop driving the *Pitx2*-governed left-sided transcriptional program that reproducibly rotates the vertebrate intestine. These findings address a long-standing question of how asymmetric organs interpret the embryonic body plan to execute local programs of laterality. Uncovering the basic mechanisms for how organs form could aid efforts to diagnose and prevent birth defects, including intestinal malrotation and volvulus, which may cause large stretches of intestinal tissue to die, a surgical emergency in neonates. Though focused on the intestine, our studies are relevant to other asymmetric organs where laterality errors also cause lethal birth defects in human babies.

Summary

The vertebrate intestine forms by asymmetric gut rotation and elongation, and errors cause lethal obstructions in human infants. Rotation begins with tissue deformation of the dorsal mesentery, which is dependent on left-sided expression of the Paired-like transcription factor *Pitx2*. The conserved morphogen *Nodal* induces asymmetric *Pitx2* to govern embryonic laterality, but organ-level regulation of *Pitx2* during gut asymmetry remains unknown. We found *Nodal* to be dispensable for *Pitx2* expression during mesentery deformation. Intestinal rotation instead required a mechanosensitive latent transforming growth factor–β (TGFβ), tuning a second wave of *Pitx2* that induced reciprocal tissue stiffness in the left mesentery as mechanical feedback with the right side. This signaling regulator, an accelerator (right) and brake (left), combines biochemical and biomechanical inputs to break gut morphological symmetry and direct intestinal rotation.

Evolutionarily conserved left-right (LR) asymmetries of vertebrate internal organs require a coordinated set of sharply defined gene expression events that drive changes in extracellular matrix (ECM) biomechanics and cell behavior. For example, the vertebrate embryonic midgut, which gives rise to most of the large and small intestine (Fig. 1A), undergoes a stereotypical counterclockwise rotation that is necessary for subsequent gut looping (1, 2). Failure to initiate midgut rotation leads to midgut volvulus, a catastrophic blockage of the gut tube and mesenteric blood vessels (3, 4). In birds and mice, the direction of midgut rotation is driven by asymmetric cellular behaviors within the dorsal mesentery (DM), the adjacent connective organ that suspends the gut tube from the dorsal body wall (Fig. 1B, colored regions), and through which intestinal blood and lymphatic vessels traverse (1, 2, 5).

The DM forms during embryogenesis by apposition and fusion of the left and right flat sheets of splanchnic mesoderm (derived from lateral plate mesoderm). This starts on day 3 in the chicken, which corresponds to Hamburger-Hamilton stage 17 (HH17) (6), or on embryonic day 9.5 (E9.5) in mice (1). Initially, the mesenchyme of the left and right splanchnic mesoderm appears homogeneous (1), but with DM formation, it develops distinct LR asymmetry where the left side condenses and the right side expands (Fig.1B, bottom panel) (1, 7, 8).The resulting deformation of the DM tilts the attached gut tube leftward, providing a critical bias for the initiation of counterclockwise gut rotation (Fig. 1B, HH21) (1, 5).

Gut rotation is directed by the transcription factor *Pitx2* (1, 9–11), which is responsible for the transfer of LR patterning information from early gastrulation to downstream organ morphogenesis (1, 5, 8, 11). *Pitx2* is expressed on the left side of the DM (Fig. 1C), where it activates pathways that regulate actin cytoskeleton organization, cell adhesion, and

ECM compaction to induce polarized condensation of the left DM (5, 8), suggesting key roles in DM morphogenesis. However, cell mechanistic studies downstream of *Pitx2* have been hampered because loss of *Pitx2* on the left causes a double right-side identity (double-right isomerism), which causes a cell fate change preventing analysis of *Pitx2*-directed morphogenesis (10).

In early embryos, *Pitx2* expression is induced in the left lateral plate mesoderm by the highly conserved morphogen *Nodal*, a member of the transforming growth factor–β (TGFβ) super-family (10, 12). This asymmetric *Nodal* expression is transient and stops before asymmetric organ morphogenesis (13, 14). However, *Pitx2* expression is present on the left side in all derivatives of the lateral plate, including the DM (Fig. 1C), and long after *Nodal* expression has ceased, leaving unresolved the question of how *Pitx2* regulates asymmetric organogenesis when *Nodal* is gone.

We found that *Pitx2* expression in the left DM required a second signaling regulator, a mechanosensitive latent transforming growth factor *β* (TGFβ), to drive gut rotation. This second wave of *Pitx2* expression repressed the initially bilateral bone morphogenetic protein 4 (*Bmp4*) expression, marking the first molecular asymmetry in the DM. Persistent BMP4 signaling within the right DM promoted mesenchymal expansion on the right. This expansion was sensed and mechanically transduced into TGFβ-dependent *Pitx2* expression changes in the left DM, resulting in polarized mesenchymal condensation and increased tissue stiffness. We further showed that the BMP antagonist Noggin simultaneously inhibits right-derived BMP4 and left-derived TGFβ-*Pitx2* activity to spatiotemporally restrict tissue deformation of the DM. This finding allowed us to uncouple the mechanosensitive role of TGFβ-*Pitx2* in asymmetric gut morphogenesis from *Pitx2*-driven laterality, a phenotype that is masked by the double right-side identity in *Pitx2*-null mice.

We propose that TGFβ-dependent control of *Pitx2* dosage on the left provides transcriptionally patterned resistance to expansion from the right. These findings can be explained by an accelerator on the right (BMP4) and a brake on the left (TGFβ-*Pitx2*), which cooperate through mechanical feedback to drive the conserved counterclockwise gut rotation.

Repression of symmetrical *Bmp4* by *Pitx2* initiates DM asymmetry

Gut rotation is first initiated by an expansion of the ECM in the right DM (Fig. 1B, bottom panel, teal) (7). This expansion and subsequent gut tilting depends on matrices of hyaluronan (HA) modified by the enzyme *Tsg6* (tumor necrosis factor-alpha–stimulated gene 6) (7), but the upstream transcriptional control of this process is unknown. Our prior transcriptomics studies performed in the chicken DM at the time of tilting (HH21) (8) revealed enrichment of *Bmp4* on the right side of the chicken DM. This raised the possibility that *Tsg6* expression and the resulting ECM expansion may be regulated by BMPs, members of the TGFβ superfamily. RNA in situ hybridization in the chicken revealed that *Bmp4* expression is initially bilateral in the DM but decreases on the left as tilting begins (Fig. 1D). We reasoned that this pattern might be governed by *Pitx2*, because loss of left-sided *Bmp4* expression coincided in space and time with the onset of *Pitx2* expression in the

left DM (Fig. 1C). This was confirmed by right-sided electroporation (fig. S1B) of *Pitx2* before chicken DM formation, which resulted in a reduction of both *Bmp4* expression (Fig. 2A) and HA accumulation on the right (Fig. 2, B and C). This double-left isomerism caused a loss of gut tilting (Fig. 2G, net-zero tilting angle from the midline measured at HH21). Co-electroporating *Pitx2* and *Bmp4* on the right rescued the right-sided program, as determined by restored HA accumulation (Fig. 2, B and C) and normal gut tilting (Fig. 2G). Thus, *Pitx2* contributes to *Bmp4* transcriptional suppression.

To more clearly define the role of right-sided BMP signaling, we electroporated the BMP antagonist *Noggin* (15–17) into the right DM. This resulted in a loss of HA accumulation (Fig. 2, C and D), *Tsg6* expression (Fig. 2D), and gut tilting (Fig. 2G). Because *Noggin* is a broad antagonist of several members of the TGFβ superfamily (15, 18), we also electroporated a dominant-negative BMP receptor 1 (*BmpR1-DN*, truncated kinase domain) (17) into the right DM. This produced a similar loss of HA (Fig. 2, C and D), *Tsg6* (Fig. 2D), and gut tilting (Fig. 2G). Perturbation of BMP signaling did not produce ectopic *Pitx2* expression in the right DM (Fig. 2E), indicating that BMP signaling independently drives the right-sided ECM expansion and not does repress the left-lateralizing *Pitx2* program.

To assess the role of *Bmp4* in the mouse embryonic midgut, *Bmp4* was conditionally deleted (fig. S2, A and B) using an inducible *Hoxb6* driver that is specifically active in the posterior lateral plate mesoderm (19). This produced a loss of HA accumulation (fig. S2C) and led to gut rotation defects evident at E12.75 (fig. S2D) without ectopic *Pitx2* expression on the right (Fig. 2H). Thus, BMP signaling independently induces *Tsg6* expression and ECM expansion of the right DM.

In mice lacking *Pitx2* (*Pitx2*$^{hd/hd}$), the left DM mesenchyme becomes expanded like the right side and gut tilting is arrested (1). To test whether *Pitx2* expression in the left DM is necessary to repress drivers of right-side identity, we examined *Bmp4* expression and HA accumulation in *Pitx2*$^{hd/hd}$ embryos at E10.5 (Fig. 2I). Both HA and *Bmp4* were present bilaterally (a double-right isomerism), indicating that *Pitx2* expression on the left represses gene expression and cell behavior normally associated with the right side of the DM. This contrasts with the loss of *Bmp4* on the right, which does not lead to bilateral *Pitx2* expression (Fig. 2H). In summary, *Pitx2* is both necessary and sufficient to inhibit BMP signaling in the DM and to specify the left-side identity of the DM.

Noggin restricts asymmetric tissue deformation to the DM

The mesenchymal cells within the DM and those within the gut tube arise from adjacent precursor populations in the left and right splanchnic mesoderm (17, 20) (Fig. 3A). LR asymmetric cell behaviors that specifically deform the DM are limited only to the DM cells and never extend ventrally into the gut tube (Fig. 3A). For example, *Smad6*, a canonical regulatory feedback gene downstream of *Bmp4* expression (21), was found strictly within the right DM and only at the onset of tilting, but never in the gut tube despite the persistence of bilateral *Bmp4* mRNA expression in the gut (fig. S1A). We reasoned that BMP signaling must be actively repressed at the protein level in the gut tube. Consistent with this idea, we initially found *Noggin* expression throughout the early left and right splanchnic

mesoderm (fig. S3A; HH15), but at the onset of DM formation, *Noggin* expression became progressively restricted to the cells of the gut tube in both chicken and mouse embryos (fig. S3, A and B). Furthermore, right-sided electroporation of constitutively active *BmpR1* (Q233D, *BmpR1-CA*) (22) into the gut splanchnic mesoderm bypassed Noggin activity and induced DM-like accumulation of HA in the gut tube (fig. S4). These data suggest that gut tube-derived Noggin limits BMP signaling–driven ECM expansion to the right DM.

The displacement of *Noggin* expression away from the forming DM was also commensurate with the onset of *Pitx2* expression on the left, suggesting a previously undescribed, antagonistic relationship between *Noggin* and *Pitx2* (fig. S3A). Indeed, electroporation of *Noggin* in the left DM caused a loss of *Pitx2* expression (Fig. 4, A and B). Moreover, mouse embryos lacking *Noggin* displayed an abnormally extended domain of *Pitx2* expression into the gut tube (fig. S3C), premature gut tilting at E9.5 (fig. S3D), and aberrant gut rotation patterns at E12.75 (fig. S3, E and F). These results indicate that gut tube–derived *Noggin* limits LR gene expression and cell behavior to the DM, shedding light on the local mechanisms that pattern molecular and morphological boundaries between the DM and the adjoining gut tube that allow timely asymmetric deformation.

Gut rotation requires a second wave of *Pitx2* expression independent of mesodermal *Nodal*

We examined *Pitx2* expression during the pre- and early DM formation periods (Fig. 3A). Early *Pitx2* expression was detected in the left splanchnic mesoderm at E8.0 (mouse) (23) and HH12 (chicken) (10, 23, 24) (Fig. 3, B and D), but was unexpectedly absent in this region shortly afterward (E9.0 mouse, Fig. 3C; HH15 chicken, Fig. 3, B and D, and fig. S3A). *Pitx2* expression was detected again as the DM began to form, both in the mouse (E9.5, Fig. 3C) and chicken (HH17, Fig. 3D and fig. S3A).

We next analyzed conditional *Nodal* mouse mutants generated with a Hoxb1-Cre driver, which ablates all *Nodal* transcription and subsequent *Pitx2* expression in the lateral plate mesoderm (25), causing heart and lung laterality defects (26). Neither gut tilting (Fig. 3E; n = 12/14) nor *Pitx2* expression in the DM (Fig. 3E; $n = 6/7$) was affected by the deletion of mesodermal *Nodal*. Thus, whereas *Nodal* drives the first wave of asymmetric *Pitx2* to govern embryonic laterality, subsequent organ-level regulation of *Pitx2* expression (second wave) during the establishment of gut-specific asymmetry may be regulated by an additional pathway.

Latent TGFβ directs gut-specific asymmetry through *Pitx2* expression

We first tested whether the second wave of *Pitx2* expression is BMP dependent (27–29), which would be consistent with the loss of *Pitx2* expression observed upon *Noggin* electroporation on the left (Fig. 4, A and B). However, electroporating *BmpR1-DN* on the left did not alter *Pitx2* expression or HA accumulation (Fig. 4, A and B), nor did it affect gut tilting (Fig. 4C), indicative of a BMP-independent mechanism to modulate *Pitx2* expression during gut rotation.

Noggin can antagonize several non-BMP TGFβ ligands (15, 18), and our DM transcriptomics data revealed that the latent TGFβ binding protein 1 (*Ltbp1*), a major regulator of TGFβ pathway activation (30, 31), is expressed strictly within the left chicken and mouse DM, akin to the spatiotemporal kinetics of *Pitx2* expression (Fig. 4D). Similarly, TGFβ-induced (*TGFβ-i*), an effector downstream of TGFβ signaling (32), was also asymmetrically expressed in the left chicken DM (fig. S5A). Thus, TGFβ activation may regulate gut-specific *Pitx2* expression and be a target for Noggin inhibition. To test this, we electroporated a kinase-defective dominant-negative TGFβRII (TGFβRII-DN) (33) on the left side. This reduced *Pitx2* expression in the DM (Fig. 4,A and B). *Pitx2* expression was similarly decreased when a dominant-negative *Ltbp1* (*Ltbp1-DN*) was electroporated into the left DM to block TGFβ activation (34) (Fig. 4, A and B). By contrast, electroporation of constitutively active TGFβRI (*TGFβ RI-CA*) (35) into the left gut splanchnic mesoderm expanded *Pitx2* expression along the gut tube primordium (Fig. 4E; HH18) and prematurely induced it at HH15 (Fig. 4F), bypassing the local presence of *Noggin* (fig. S4A). We also inserted resin beads into the left coelomic cavity (fig. S1C) (7, 11) that were coated with a TGFβ receptor type 1 (TGFβ RI) inhibitor (SB431542) (36) or a more specific TGFβ RI and RII dual inhibitor (LY2109761) (37). In both cases, *Pitx2* expression was significantly reduced in response to TGFβ inhibition (Fig. 5, A and B). Finally, explants isolated from mouse intestine and cultured with LY2109761 had reduced *Pitx2* expression and perturbed gut rotation (fig. S5B).

Gain of function of BMP4 on the left masks morphogenetic phenotypes of *Pitx2* loss

Genetic loss of all *Pitx2* expression in mice results in a DM with a double right-side isomerism and loss of gut tilting because BMP4 inhibition is lost on the left (Fig. 4G, panels 1 to 4). Similarly, electroporating *TGFβ RII-DN* or *Ltbp1-DN* caused a nearly complete loss of *Pitx2* expression (Fig. 4, A and B), resulting in bilateral activation of BMP4-mediated HA accumulation (Fig. 4A) and loss of gut tilting (Fig. 4C), identical to *Pitx2*-null mice. However, inhibiting *Pitx2* expression by electroporating Noggin in chicken embryos does not result in a double-right DM because Noggin also inhibits BMP4 and HA accumulation (no double-right isomerism; Fig. 4A). In such Noggin-expressing *Pitx2*-lacking embryos, the left-sided rotation (tilting angle) was increased (“over-tilting”; Fig. 4, A, C, and G, panels 1, 4, and 5). Similarly, perturbing TGFβ activation with drugs that reduced *Pitx2* expression caused the same over-tilting (Figs. 5, A to C, and 4G, panel 6). Thus, the over-tilting phenotype appears to result from an absence or reduction of *Pitx2* expression on the left, but can be revealed only when there is no accompanying double-right conversion. We conclude that *Pitx2* has two distinct roles in gut asymmetry: (i) it specifies the left side by suppressing *Bmp4* expression and (ii) it directs morphogenesis of gut tilting downstream of TGFβ activation (Fig. 4G).

The contractile status of the DM is mechanically sensed by TGFβ-*Pitx2*

TGFβ becomes active when liberated from the latent complex that is covalently linked to ECM-resident Ltbp1 (30, 38, 39). Several mechanisms induce conformational changes

of the latent complex, including the contractile force of cells (38–41) and mechanical tissue stretch in vitro and in vivo (42–45), leading to the release of TGFβ from the ECM (46). To test whether *Pitx2* expression in the DM responds to mechanical stress through mechanosensitive TGFβ release, we subjected slices of the DM and gut tissue to physical stretches of up to 20% (fig. S6A) (47). Stretching these slices resulted in increased (free) TGFβ (pan-TGFβ) protein (fig. S6B). This was accompanied by increased *Pitx2* expression on the left side of the DM that was proportional to the stretch applied (fig. S6C).

To test Pitx2 mechanosensitivity in vivo, we targeted the left coelomic cavity with resin beads soaked in blebbistatin, an inhibitor of nonmuscle myosin II ATPase (48). This decreased *Pitx2* expression in the left DM by >50% (Fig. 5, A and B) and increased the tilting angle (Fig. 5, A and C), a phenotype similar to that obtained after pharmacologic TGFβ inhibition (Fig. 5, A to C). By contrast, beads soaked with calyculin A, which activates myosin II and increases contractile force (49), increased *Pitx2* expression and decreased gut tilting (Fig. 5, A to C). A combination of blebbistatin and calyculin A restored both *Pitx2* expression and gut tilting (Fig. 5, A to C). We also electroporated a photoactivatable myosin light chain kinase (MLCK) inhibitor (PA-MKI), a more specific inhibitor of myosin II (50), allowing precise temporal disruption of contractility in the left DM after the establishment of molecular LR asymmetry. This decreased *Pitx2* expression (Fig. 5, D and E) and increased the tilting angle (Fig. 5, D and F). Co-electroporating PA-MKI and TGFβ RI-CA rescued *Pitx2* expression and partially restored gut tilting (Fig. 5, D to F). Thus, direct modulation of contractility in the DM is sufficient to alter *Pitx2* mRNA expression through latent release of TGFβ. Quantitative analyses of the above perturbations confirmed the mechano-sensitivity of *Pitx2* abundance and the inverse relationship between *Pitx2* expression levels and the degree of gut tilting (Fig. 5G).

Pitx2 induces polarized condensation on the left by mechanical feedback with the right

A second wave of *Pitx2* expression is observed at the onset of DM formation, but this expression is further increased commensurate with expansion on the right, which might reflect mechanical feedback (Fig.1C). Moreover, *Pitx2* drives polarized condensation on the left shortly after expansion on the right (7). Thus, we tested whether forces deriving initially from the right-side expansion might drive mechanical TGFβ ligand release and *Pitx2* dosage on the left, tightly regulating and polarizing mesenchymal condensation in response to expansion. This model would explain how *Pitx2* reduction on the left would impair the (active) responses to expansion on the right, causing deregulated (passive) over-tilting.

To test this model in vivo, we inhibited expansion and gut tilting by electroporating chicken embryos with hyaluronidase 2 (*Hyal2*) to degrade extracellular HA (7). To allow precise temporal manipulation of expansion after the establishment of molecular LR asymmetry, we used the tetracycline (Tet)-on inducible chicken expression construct TRE-EGFP for these experiments (51). Loss of expansion on the right decreased *Pitx2* expression on the left (Fig. 6, A and B). Conversely, we exaggerated ECM expansion by electroporating *Tsg6* with HA synthase 2 (*Has2*) into the right DM (7) (Fig. 6, A and E). Ectopic *Tsg6* plus *Has2*

increased expansion on the right and significantly increased condensation of the neighboring left DM (Fig. 6E). Increased expansion also increased accumulation of free TGFβ protein (Fig. 6D) and *Pitx2* expression (Fig. 6 A and B). Thus, we propose an "accelerator-brake" model in which right-sided ECM expansion acts as an accelerator of gut rotation, whereas TGFβ- *pitx2*–directed mesenchymal condensation on the left acts as a brake to inhibit rotation. Consistent with this model, direct overexpression of *TGFβRI-CA*, *Pitx2*, or the constitutively active form of the Pitx2 effector Daam2 (Daam2-CA) (8) on the left resulted in reduced gut tilting (Fig. 4C). Moreover, over-tilting caused by Noggin-induced loss of *Pitx2* expression (absence of brake) was associated with a loss of mesenchymal cell polarity within the left DM, as measured by the orientation of the Golgi apparatus (8) relative to the nucleus (fig. S7A). Disorganized condensation in the absence of polarity also resulted in the clumping of actin fibers (fig. S7B) in crowded areas, which was never observed during the wild-type *Pitx2*-driven condensation program (fig. S7B) (8) or during the mechanically exacerbated wild-type *Pitx2* program induced by the right-sided *Tsg6* plus *Has2* co-electroporation (fig. S7B). We interpret this to mean that mesenchymal cell crowding in the absence of *Pitx2* is a deregulated consequence of right-sided expansion (passive left-side compaction) as opposed to *Pitx2*-patterned (active) polarized condensation in response to expansion.

Pitx2 patterns DM stiffness on the left to resist right-side generated forces

Tissue deformation reflects a balance of forces and stiffness (52). We hypothesized that polarized condensation stiffens the left side, which resists right side–generated forces. To test whether gut tilting results from a combination of unequal forces and stiffness across the LR axis of the DM, we performed direct measurements of DM tissue stiffness during gut tilting using a microindentation system (Chiaro nanoindenter) (Fig. 6F). These studies revealed that the condensed left side of the wild-type DM was significantly stiffer than the hydrated nature of the HA matrix on the right side, whereas the gut tube had uniform intermediate stiffness (Fig. 6F and fig. S8). Ectopic expression of *Pitx2* on the right side stiffened the ECM, approximating the stiffness of the left side of the wild-type DM (Fig. 6F). Moreover, Noggin-induced loss of *Pitx2* expression on the left caused a loss in tissue stiffness of that side, resulting in tissue stiffness approximating that of the right side (Fig. 6F). Thus, *Pitx2* is necessary and sufficient to regulate DM stiffness during gut tilting.

After exaggerating expansion on the right (with *Tsg6* plus *Has2*), the soft hydrated HA-rich ECM became even softer and the left side became stiffer (Fig. 6F), reflecting the consequential increase in TGFβ (Fig. 6D) and *Pitx2* expression on the left (Fig. 6, A and B). These changes did not significantly alter the overall gut tilting (Fig. 6C), reinforcing the importance of the mechanical feedback loop in balancing gut tilting. Our results show that the left-sided latent TGFβ complex responds to mechanical stress from the expanding right side and amplifies *Pitx2* expression, which in turn stiffens the left side through polarized condensation of the mesenchyme, tuning a second wave of *Pitx2* expression. Thus, our accelerator-brake model incorporates both biochemical and biomechanical inputs to cooperatively drive and steer the crucial counterclockwise rotation of the embryonic midgut (Fig. 6G).

As an additional test of our model, we predicted that we could reverse the conserved gut tilting by misexpression of the wild-type *Pitx2* on the right and TGFβRII-DN on the left to inhibit *Pitx2* expression. Indeed, gain of function of *Pitx2* on the right and loss of the left-sided TGFβ signaling reversed gut tilting (fig. S9).

Discussion

Pitx2 functions in both establishing LR asymmetry and translating this laterality to morphogenesis of the internal organs. However, it remains unresolved how *Pitx2* expression modifies cell behavior and how this is regulated within local, organ-specific microenvironments. In the DM, these events are characterized by an expansion of the right-side mesenchyme, which is driven by BMP-induced accumulation of HA; this expansion is accompanied by mesenchymal compaction on the left side. These asymmetries produce the characteristic counterclockwise gut rotation found in most vertebrates.

Pitx2 expression during broad specification of axial chirality and the later execution of asymmetric tissue changes appear to be controlled by different regulatory pathways (Fig. 7, A and B). In the lateral plate mesoderm, *Nodal* induces the first wave of *Pitx2* expression on the left to govern embryonic laterality (Fig. 7A). In the DM, a second wave of *Pitx2* expression is controlled by the mechanosensitive TGFβ latency complex on the left (Fig. 7B). Deletion of *Nodal* from the lateral plate mesoderm preserved wild-type *Pitx2* expression ($n = 6/7$) and gut laterality ($n = 12/14$). Thus, whereas early *Nodal* expression at the node, the mouse signaling center where symmetry is first broken, is essential to specifying the embryonic LR body plan (12, 53, 54), further changes in local intestinal asymmetry can be uncoupled from *Nodal* transcription in the lateral plate mesoderm. The incomplete penetrance of correct gut rotation (two of 14 embryos rotated to the right with right-sided *Pitx2*) suggests that *Nodal* may be important to ensure the robust alignment of organ-level laterality with the LR body axis. Neither electroporation of *Nodal* nor TGFβRI-CA in the right splanchnic mesoderm was sufficient to induce bilateral *Pitx2* expression in the DM (fig. S10), reinforcing that local amplification of gut-specific *Pitx2* expression requires prior laterality information established during early embryogenesis. Thus, our study supports a two-step model of asymmetric organogenesis (55), and our findings support the presence of additional mechanisms through which laterality information is delivered to individual organ primordia.

We observed that Noggin is produced by splanchnic mesoderm surrounding the gut tube, and progressive distancing of the Noggin^{+} gut tube primordium from the Noggin^{-} cells of the DM may affect the timely activation of DM-specific LR programs (Fig. 7, A and B). Indeed, Noggin not only antagonizes BMP4 signaling within the right DM but also inhibits TGFβ-*Pitx2* activity on the left. This revealed a separate role for *Pitx2* in governing the mechanical properties of the DM, in which the forces generated by an adjoining tissue (right DM) are converted into a transcriptional response (*Pitx2* expression) through mechanical activation of the latent TGFβ complex (Fig. 7C), a phenomenon previously observed in cancer and fibrosis (46). Our data reveal that material properties across the LR axis of the DM, including tissue stiffness, determine the extent of deformation during gut rotation, a process patterned by *Pitx2* and executed by TGFβ and BMP4.

Ltbp1, the major regulator of latent TGFβ activation, is transcribed asymmetrically on the left side commensurate with *Pitx2* expression, which presumably enhances TGFβ release and activation on the left (Fig. 7, B and C). The LTBP family of proteins are expressed in restricted tissue types to provide specificity to TGFβ ligands that have widespread expression (46). This diversity is further expanded by the variety of stresses that can cause TGFβ release, including mechanical forces, pH, reactive oxygen species, and matrix metalloproteinases (46). Our findings in the DM reveal that mechanical forces propagate TGFβ-*Pitx2* signaling in the mechanically condensed left DM, but other stimuli may also participate. TGFβ and BMP signaling also function in LR asymmetric gut bending in sea urchin embryos, suggesting an evolutionarily ancient mechanism for gut-specific asymmetry (56).

Funding:

This work was supported by the National Institute of Diabetes and Digestive and Kidney Diseases (grants R01 DK092776 and R01 DK107634 to N.A.K.); the March of Dimes (grant 1-FY11-520 to N.A.K.); the National Heart, Lung and Blood Institute (grant R01 HL082792 to J.L.); the Volkswagen Foundation (J.L.); the Cornell Center for Vertebrate Genomics Scholarship (B.D.S.); and the National Institutes of Health (grant 1S10RR025502 to the Cornell Institute of Biotechnology).

Supplementary Material

Refer to Web version on PubMed Central for supplementary material.

ACKNOWLEDGMENTS

We thank J. Liu, D. Gludish, D. Noden, and members of the Kurpios lab for suggestions on the manuscript; A. Desgrange and S. Meilhac for the production of *Nodal* mutant mouse embryos and critical feedback; R. Harland for the Noggin-null mouse; S. Mackem for the Hoxb6 CreERT mice; T. Schultheiss, A. Bandyopadyay, C. Tabin, C. Cepko, C. Krull, L. Niswander, P. ten Dijke, J. Massague, J. Wrana, A. Moustakas, and P. Brickell for plasmids; and C. Demler, R. Slater, F. Lee, B. Laslow, A. Sivakumar, C. Harris, M. Simoes-Costa, and the Cornell Imaging Facility for technical assistance.

REFERENCES AND NOTES

1. Davis NM et al. , The chirality of gut rotation derives from left-right asymmetric changes in the architecture of the dorsal mesentery. Dev. Cell 15, 134–145 (2008). doi: 10.1016/j.devcel.2008.05.001; pmid: [PubMed: 18606147]
2. Savin T. et al. , On the growth and form of the gut. Nature 476, 57–62 (2011). doi: 10.1038/nature10277; pmid: [PubMed: 21814276]
3. Shalaby MS, Kuti K, Walker G, Intestinal malrotation and volvulus in infants and children. BMJ 347 (nov26 2), f6949 (2013). doi: 10.1136/bmj.f6949; pmid: [PubMed: 24285798]
4. Applegate KE, Evidence-based diagnosis of malrotation and volvulus. Pediatr. Radiol. 39 (Suppl 2), S161–S163 (2009). doi: 10.1007/s00247-009-1177-x; pmid: [PubMed: 19308378]
5. Kurpios NA et al. , The direction of gut looping is established by changes in the extracellular matrix and in cell:cell adhesion. Proc. Natl. Acad. Sci. U.S.A 105, 8499–8506 (2008). doi: 10.1073/pnas.0803578105; pmid: [PubMed: 18574143]
6. Hamburger V, Hamilton HL, A series of normal stages in the development of the chick embryo. J. Morphol 88, 49–92 (1951). pmid: [PubMed: 24539719]

7. Sivakumar A. et al. , Midgut laterality is driven by hyaluronan on the right. Dev. Cell 46, 533–551.e5 (2018). doi: 10.1016/j.devcel.2018.08.002; pmid: [PubMed: 30174180]
8. Welsh IC et al. , Integration of left-right Pitx2 transcription and Wnt signaling drives asymmetric gut morphogenesis via Daam2. Dev. Cell 26, 629–644 (2013). doi: 10.1016/j.devcel.2013.07.019; pmid: [PubMed: 24091014]
9. Lu MF, Pressman C, Dyer R, Johnson RL, Martin JF, Function of Rieger syndrome gene in left-right asymmetry and craniofacial development. Nature 401, 276–278 (1999). doi: 10.1038/45797; pmid: [PubMed: 10499585]
10. Logan M, Pagán-Westphal SM, Smith DM, Paganessi L, Tabin CJ, The transcription factor Pitx2 mediates situs-specific morphogenesis in response to left-right asymmetric signals. Cell 94, 307–317 (1998). doi: 10.1016/S0092-8674(00)81474-9; pmid: [PubMed: 9708733]
11. Mahadevan A. et al. , The left-right Pitx2 pathway drives organ-specific arterial and lymphatic development in the intestine. Dev. Cell 31, 690–706 (2014). doi: 10.1016/j.devcel.2014.11.002; pmid: [PubMed: 25482882]
12. Levin M, Johnson RL, Stern CD, Kuehn M, Tabin C, A molecular pathway determining left-right asymmetry in chick embryogenesis. Cell 82, 803–814 (1995). doi: 10.1016/0092-8674(95)90477-8; pmid: [PubMed: 7671308]
13. Logan M, Tabin C, Targeted gene misexpression in chick limb buds using avian replication-competent retroviruses. Methods 14, 407–420 (1998). doi: 10.1006/meth.1998.0595; pmid: [PubMed: 9608511]
14. Ryan AK et al. , Pitx2 determines left-right asymmetry of internal organs in vertebrates. Nature 394, 545–551 (1998). doi: 10.1038/29004; pmid: [PubMed: 9707115]
15. Zimmerman LB, De Jesús-Escobar JM, Harland RM, The Spemann organizer signal noggin binds and inactivates bone morphogenetic protein 4. Cell 86, 599–606 (1996). doi: 10.1016/S0092-8674(00)80133-6; pmid: [PubMed: 8752214]
16. Groppe J. et al. , Structural basis of BMP signalling inhibition by the cystine knot protein Noggin. Nature 420, 636–642 (2002). doi: 10.1038/nature01245; pmid: [PubMed: 12478285]
17. Arraf AA, Yelin R, Reshef I, Kispert A, Schultheiss TM, Establishment of the visceral embryonic midline is a dynamic process that requires bilaterally symmetric BMP signaling. Dev. Cell 37, 571–580 (2016). doi: 10.1016/j.devcel.2016.05.018; pmid: [PubMed: 27326934]
18. Bayramov AV et al. , Novel functions of Noggin proteins: Inhibition of Activin/Nodal and Wnt signaling. Development 138, 5345–5356 (2011). doi: 10.1242/jcs.105031; pmid: [PubMed: 22071106]
19. Nguyen MT, Zhu J, Nakamura E, Bao X, Mackem S, Tamoxifen-dependent, inducible Hoxb6CreERT recombinase function in lateral plate and limb mesoderm, CNS isthmic organizer, posterior trunk neural crest, hindgut, and tailbud. Dev. Dyn 238, 467–474 (2009). doi: 10.1002/dvdy.21846; pmid: [PubMed: 19161221]
20. Thomason RT, Bader DM, Winters NI, Comprehensive timeline of mesodermal development in the quail small intestine. Dev. Dyn 241, 1678–1694 (2012). doi: 10.1002/dvdy.23855; pmid: [PubMed: 22930586]
21. Goto K, Kamiya Y, Imamura T, Miyazono K, Miyazawa K, Selective inhibitory effects of Smad6 on bone morphogenetic protein type I receptors. J. Biol. Chem 282, 20603–20611 (2007). doi: 10.1074/jbc.M702100200; pmid: [PubMed: 17493940]
22. Raja E. et al. , The protein kinase LKB1 negatively regulates bone morphogenetic protein receptor signaling. Oncotarget 7, 1120–1143 (2016). doi: 10.18632/oncotarget.6683; pmid: [PubMed: 26701726]
23. Shiratori H. et al. , Two-step regulation of left-right asymmetric expression of Pitx2: Initiation by nodal signaling and maintenance by Nkx2. Mol. Cell 7, 137–149 (2001). doi: 10.1016/S1097-2765; pmid: [PubMed: 11172719]
24. Saijoh Y. et al. , Left-right asymmetric expression of lefty2 and nodal is induced by a signaling pathway that includes the transcription factor FAST2. Mol. Cell 5, 35–47 (2000). doi: 10.1016/S1097-2765(00)80401-3; pmid: [PubMed: 10678167]

25. Forlani S, Lawson KA, Deschamps J, Acquisition of Hox codes during gastrulation and axial elongation in the mouse embryo. Development 130, 3807–3819 (2003). doi: 10.1242/dev.00573; pmid: [PubMed: 12835396]
26. Desgrange A, Le Garrec JF, Bernheim S, Bønnelykke TH,Meilhac SM, Transient nodal signaling in left precursors coordinates opposed asymmetries shaping the heart loop. Dev. Cell 55, 413–431.e6 (2020). doi: 10.1016/j.devcel.2020.10.008; pmid: [PubMed: 33171097]
27. Monsoro-Burq A, Le Douarin NM, BMP4 plays a key role in left-right patterning in chick embryos by maintaining Sonic Hedgehog asymmetry. Mol. Cell 7, 789–799 (2001). doi: 10.1016/S1097-2765(01)00223-4; pmid: [PubMed: 11336702]
28. Veerkamp J. et al. , Unilateral dampening of Bmp activity by nodal generates cardiac left-right asymmetry. Dev. Cell 24, 660–667 (2013). doi: 10.1016/j.devcel.2013.01.026; pmid: [PubMed: 23499359]
29. Ocaña OH et al. , A right-handed signalling pathway drives heart looping in vertebrates. Nature 549, 86–90 (2017). doi: 10.1038/nature23454; pmid: [PubMed: 28880281]
30. Miyazono K, Olofsson A, Colosetti P, Heldin CH, A role of the latent TGF-β 1-binding protein in the assembly and secretion of TGF-β 1. EMBO J 10, 1091–1101 (1991). doi: 10.1002/j.1460-2075.1991.tb08049.x; pmid: [PubMed: 2022183]
31. Annes JP, Munger JS, Rifkin DB, Making sense of latent TGFbeta activation. J. Cell Sci 116, 217–224 (2003). doi: 10.1242/jcs.00229; pmid: [PubMed: 12482908]
32. Skonier J. et al. , β ig-h3: A transforming growth factor-β-responsive gene encoding a secreted protein that inhibits cell attachment in vitro and suppresses the growth of CHO cells in nude mice. DNA Cell Biol 13, 571–584 (1994). doi: 10.1089/dna.1994.13.571; pmid: [PubMed: 8024701]
33. Wrana JL et al. , TGF β signals through a heteromeric protein kinase receptor complex. Cell 71, 1003–1014 (1992). doi: 10.1016/0092-8674(92)90395-S; pmid: [PubMed: 1333888]
34. Annes JP, Chen Y, Munger JS, Rifkin DB, Integrin alphaVbeta6-mediated activation of latent TGF-β requires the latent TGF-β binding protein-1. J. Cell Biol 165, 723–734 (2004). doi: 10.1083/jcb.200312172; pmid: [PubMed: 15184403]
35. Morén A, Imamura T, Miyazono K, Heldin CH, Moustakas A, Degradation of the tumor suppressor Smad4 by WW and HECT domain ubiquitin ligases. J. Biol. Chem 280, 22115–22123 (2005). doi: 10.1074/jbc.M414027200; pmid: [PubMed: 15817471]
36. Inman GJ et al. , SB-431542 is a potent and specific inhibitor of transforming growth factor-β superfamily type I activin receptor-like kinase (ALK) receptors ALK4, ALK5, and ALK7. Mol. Pharmacol 62, 65–74 (2002). doi: 10.1124/mol.62.1.65; pmid: [PubMed: 12065756]
37. Melisi D. et al. , LY2109761, a novel transforming growth factor β receptor type I and type II dual inhibitor, as a therapeutic approach to suppressing pancreatic cancer metastasis. Mol. Cancer Ther 7, 829–840 (2008). doi: 10.1158/1535-7163. MCT-07–0337; pmid: [PubMed: 18413796]
38. Wipff PJ, Rifkin DB, Meister JJ, Hinz B, Myofibroblast contraction activates latent TGF-β1 from the extracellular matrix. J. Cell Biol 179, 1311–1323 (2007). doi: 10.1083/jcb.200704042; pmid: [PubMed: 18086923]
39. Buscemi L. et al. , The single-molecule mechanics of the latent TGF-β1 complex. Curr. Biol 21, 2046–2054 (2011). doi: 10.1016/j.cub.2011.11.037; pmid: [PubMed: 22169532]
40. Giacomini MM, Travis MA, Kudo M, Sheppard D, Epithelial cells utilize cortical actin/myosin to activate latent TGF-β through integrin α(v)β(6)-dependent physical force. Exp. Cell Res 318, 716–722 (2012). doi: 10.1016/j.yexcr.2012.01.020;pmid: [PubMed: 22309779]
41. Henderson NC et al. , Targeting of αv integrin identifies a core molecular pathway that regulates fibrosis in several organs. Nat. Med 19, 1617–1624 (2013). doi: 10.1038/nm.3282;pmid: [PubMed: 24216753]
42. Sakata R, Ueno T, Nakamura T, Ueno H, Sata M, Mechanical stretch induces TGF-beta synthesis in hepatic stellate cells. Eur. J. Clin. Invest 34, 129–136 (2004). doi: 10.1111/j.1365-2362.2004.01302.x; pmid: [PubMed: 14764076]
43. Hamzeh MT, Sridhara R, Alexander LD, Cyclic stretch-induced TGF-β1 and fibronectin expression is mediated by β1-integrin through c-Src- and STAT3-dependent pathways in renal epithelial cells. Am. J. Physiol. Renal Physiol 308, F425–F436 (2015). doi: 10.1152/ajprenal.00589.2014;pmid: [PubMed: 25477471]

44. Froese AR et al. , Stretch-induced activation of transforming growth factor-β1 in pulmonary fibrosis. Am. J. Respir. Crit. Care Med 194, 84–96 (2016). doi: 10.1164/rccm.201508-1638OC; pmid: [PubMed: 26771871]
45. Walker M, Godin M, Pelling AE, Mechanical stretch sustains myofibroblast phenotype and function in microtissues through latent TGF-β1 activation. Integr. Biol 12, 199–210 (2020). doi: 10.1093/intbio/zyaa015; pmid: [PubMed: 32877929]
46. Robertson IB, Rifkin DB, Regulation of the Bioavailability of TGF-β and TGF-β-Related Proteins. Cold Spring Harb. Perspect. Biol 8, a021907 (2016). doi: 10.1101/cshperspect.a021907; pmid: [PubMed: 27252363]
47. Lombardi ML, Zwerger M, Lammerding J, Biophysical assays to probe the mechanical properties of the interphase cell nucleus: Substrate strain application and microneedle manipulation. J. Vis. Exp (55): 3087 (2011). doi: 10.3791/3087; pmid: [PubMed: 21946671]
48. Zhang M, Rao PV, Blebbistatin, a novel inhibitor of myosin II ATPase activity, increases aqueous humor outflow facility in perfused enucleated porcine eyes. Invest. Ophthalmol. Vis. Sci 46, 4130–4138 (2005). doi: 10.1167/iovs.05-0164; pmid: [PubMed: 16249490]
49. Suzuki A, Itoh T, Effects of calyculin A on tension and myosin phosphorylation in skinned smooth muscle of the rabbit mesenteric artery. Br. J. Pharmacol 109, 703–712 (1993). doi: 10.1111/j.1476-5381.1993.tb13631.x; pmid: [PubMed: 8395295]
50. Yi JJ, Wang H, Vilela M, Danuser G, Hahn KM, Manipulation of endogenous kinase activity in living cells using photoswitchable inhibitory peptides. ACS Synth. Biol 3, 788–795 (2014). doi: 10.1021/sb5001356; pmid: [PubMed: 24905630]
51. Watanabe T. et al. , Tet-on inducible system combined with in ovo electroporation dissects multiple roles of genes in somitogenesis of chicken embryos. Dev. Biol 305, 625–636 (2007). doi: 10.1016/j.ydbio.2007.01.042; pmid: [PubMed: 17359965]
52. Petridou NI, Heisenberg C-P, Tissue rheology in embryonic organization. EMBO J 38, e102497 (2019). doi: 10.15252/embj.2019102497; pmid: [PubMed: 31512749]
53. Brennan J, Norris DP, Robertson EJ, Nodal activity in the node governs left-right asymmetry. Genes Dev 16, 2339–2344 (2002). doi: 10.1101/gad.1016202; pmid: [PubMed: 12231623]
54. Saijoh Y, Oki S, Ohishi S, Hamada H, Left-right patterning of the mouse lateral plate requires nodal produced in the node. Dev. Biol 256, 160–172 (2003). doi: 10.1016/S0012-1606(02)00121-5; pmid: [PubMed: 12654299]
55. Brown NA, Wolpert L, The development of handedness in left/right asymmetry. Development 109, 1–9 (1990). doi: 10.1242/dev.109.1.1; pmid: [PubMed: 2209459]
56. Suzuki H, Yaguchi S, Transforming growth factor-β signal regulates gut bending in the sea urchin embryo. Dev. Growth Differ 60, 216–225 (2018). doi: 10.1111/dgd.12434; pmid: [PubMed: 29878318]

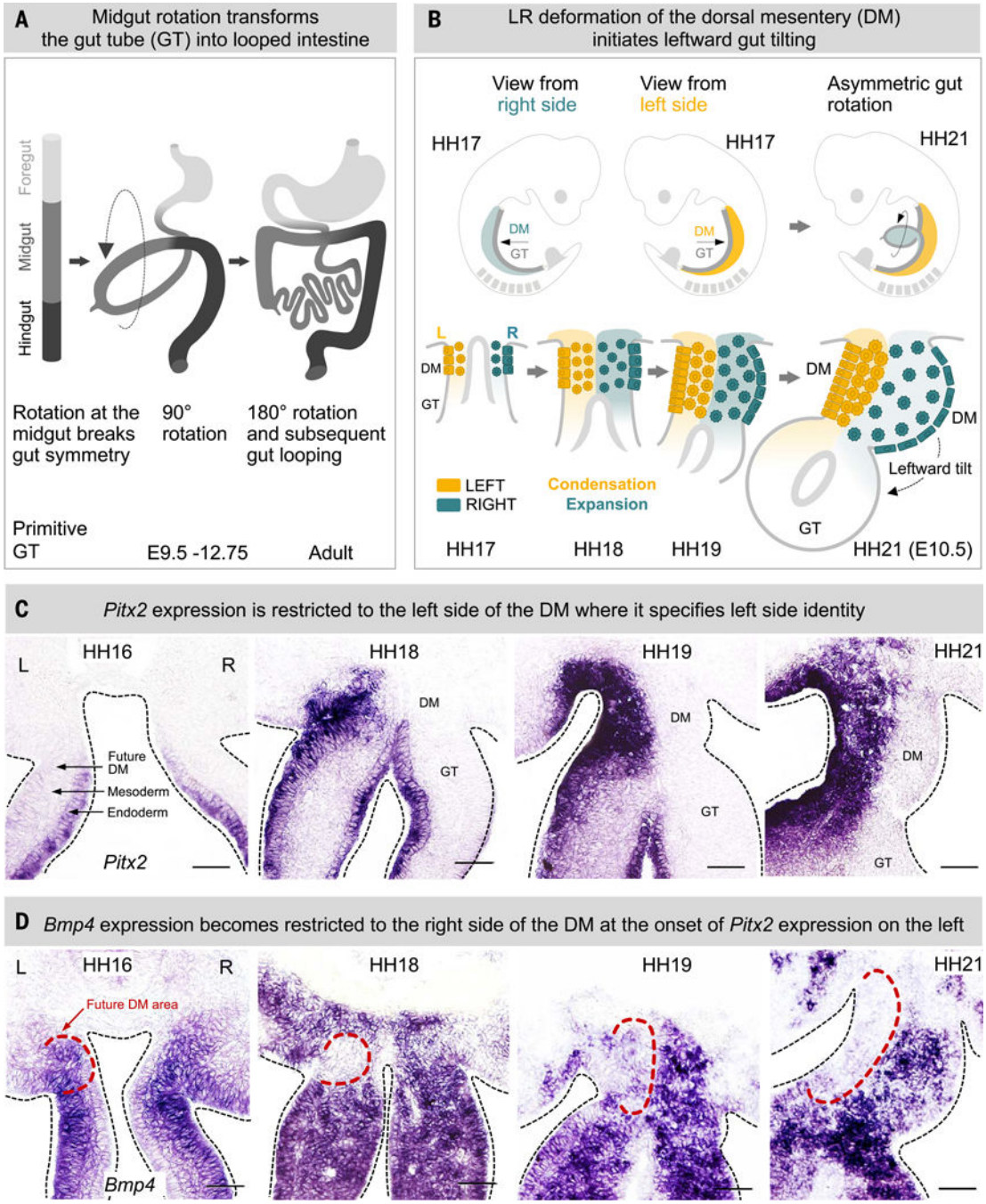

Fig. 1. BMP4 becomes restricted to the right at the onset of *Pitx2* expression on the left.

(A) Midgut rotation transforms the gut tube into looped intestine. **(B)** Tissue changes across the LR DM initiate gut tube (GT) rotation. (**C** and **D**) RNA in situ hybridization (ISH) for *Bmp4* and *Pitx2* during DM formation and GT rotation. Scale bars, 50 μm.

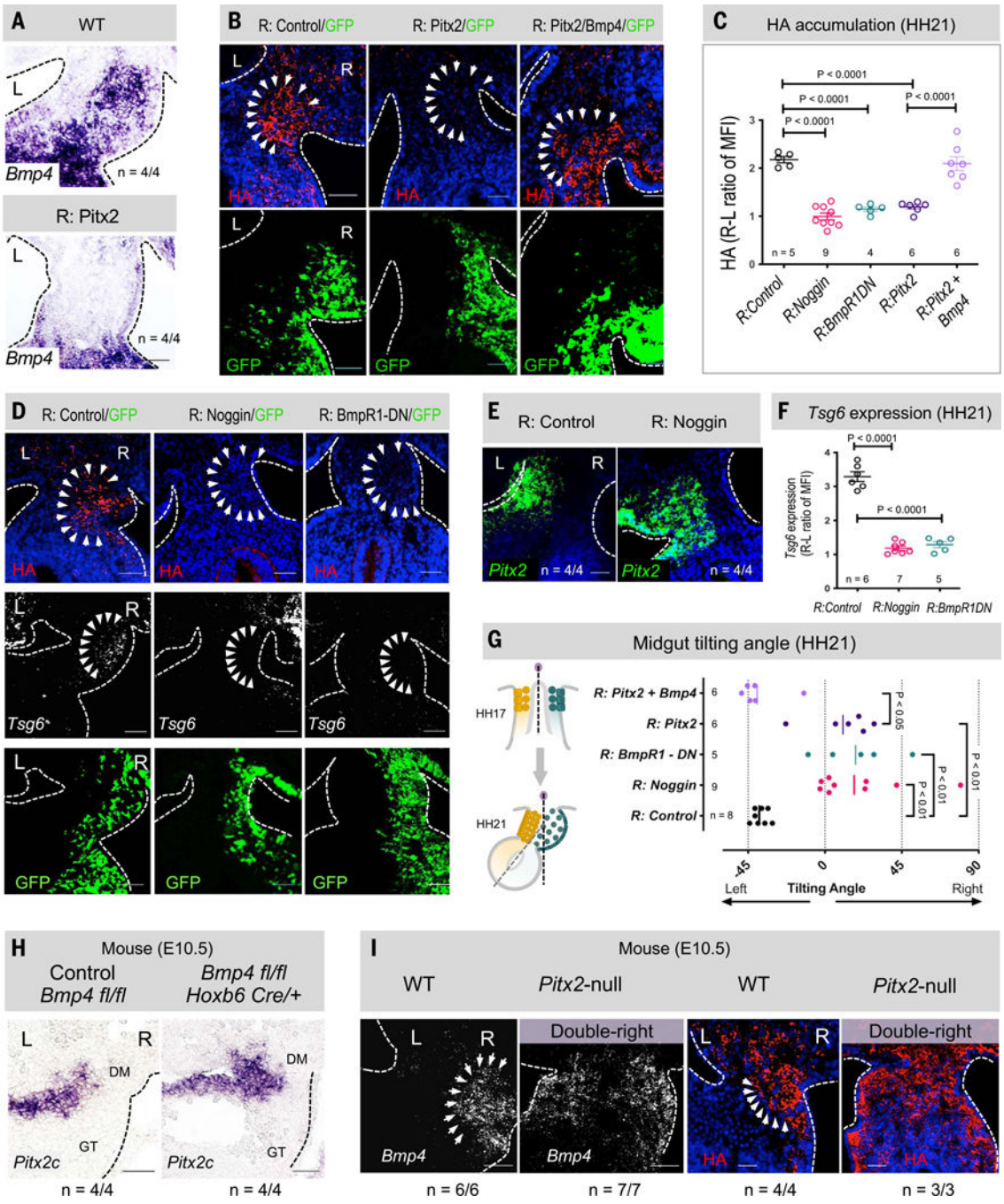

Fig. 2. BMP4 drives morphological DM asymmetry through the *Tsg6*/HA pathway.

Right-sided *Pitx2* electroporation in the chicken DM inhibits *Bmp4* expression [(**A**), ISH], HA accumulation [(**B**) in red, and quantified in (C)], and gut tilting [quantified in (G)], whereas right-sided Pitx2 with Bmp4 co-electroporation restored the right-sided program (HH21). Effect of right-sided *Noggin* or *BmpR1-DN* electroporation (HH21) on HA [(**D**) in red, and quantified in (C)] and *Tsg6* [RNAScope, (D) in white and quantified in (F)] and *Pitx2* [RNAScope, (**E**) in green]. Data were analyzed with one-way ANOVA and multiple comparisons with Tukey's correction for HA (**C**) and *Tsg6* (**F**) (presented as mean ±

SEM), and Watson's test for tilting angles (**G**) (presented as circular mean) upon specified electroporations marked by GFP. (**H** and **I**) Mouse *Pitx2c* [(H), ISH] was not affected upon *Bmp4* deletion, whereas *Pitx2* loss (I) caused a "double-right" phenotype, including ectopic HA and *Bmp4* (RNAScope). MFI, mean fluorescence intensity. All scale bars, 50 μm.

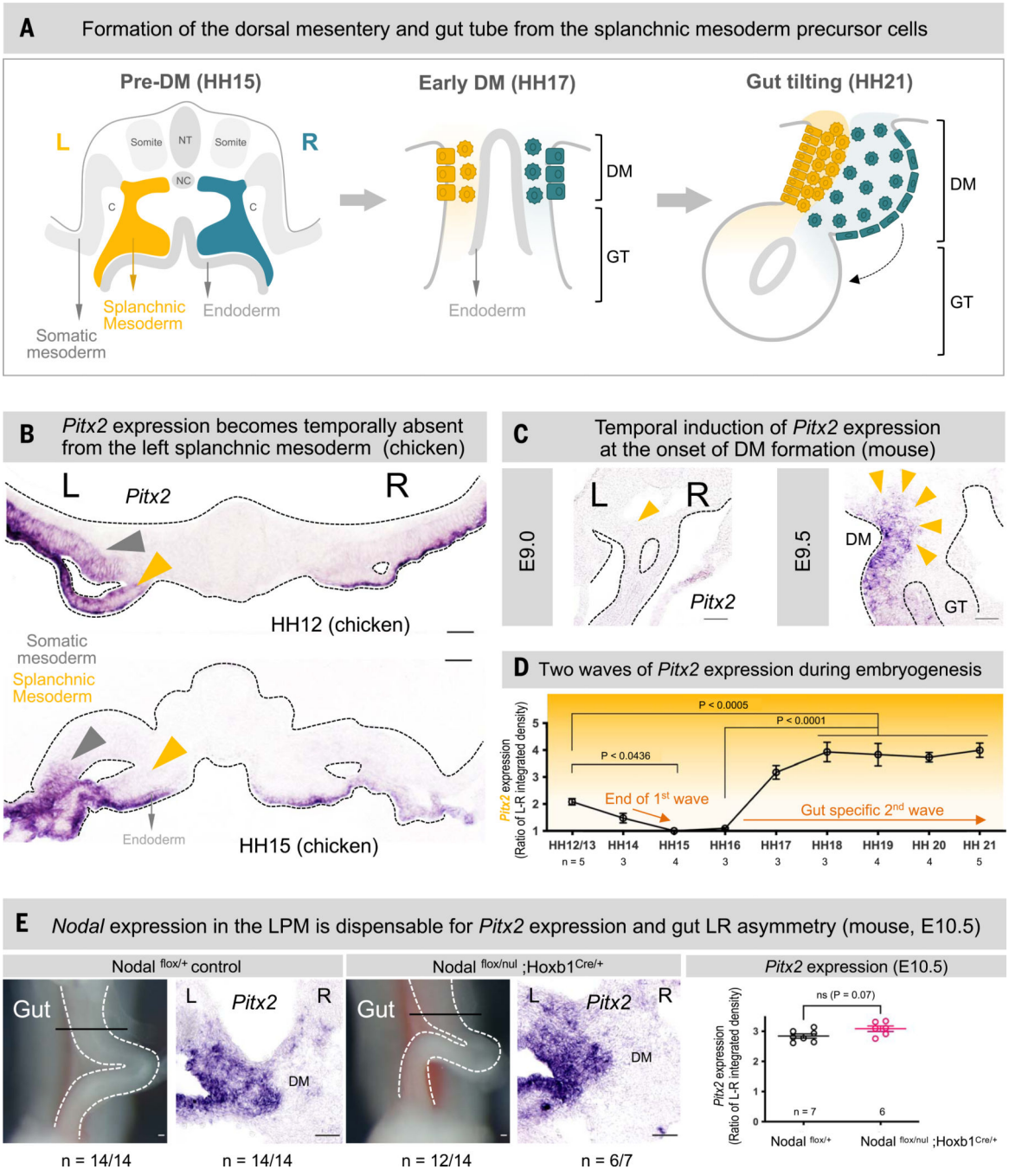

Fig. 3. Gut rotation requires a second wave of *Pitx2* independently of mesodermal *Nodal*.

(**A**) DM forms by fusion of the left and right splanchnic mesoderm; fusion of the somatic mesoderm forms the body wall. Subsequent LR tissue changes are specific to the DM and never extend ventrally into the GT. NT, neural tube; NC, notochord, C, coelom. (**B**) *Pitx2* (ISH) is expressed in the splanchnic mesoderm at HH12 but is absent at HH15 before DM formation. (**C**) In mice, *Pitx2c* is lost by E9.0 but reemerges with DM formation at E9.5. (**D**) Two waves of *Pitx2* expression quantified by integrated density normalized to somatic mesoderm, using one-way ANOVA followed by multiple comparisons with

Tukey's correction (presented as mean ± SEM). (**E**) Mouse gut tilting and *Pitx2c* expression (compared by unpaired *t* test, presented as mean ± SEM) are not perturbed by conditional *Nodal* deletion (E10.5). Scale bars, 50 μm.

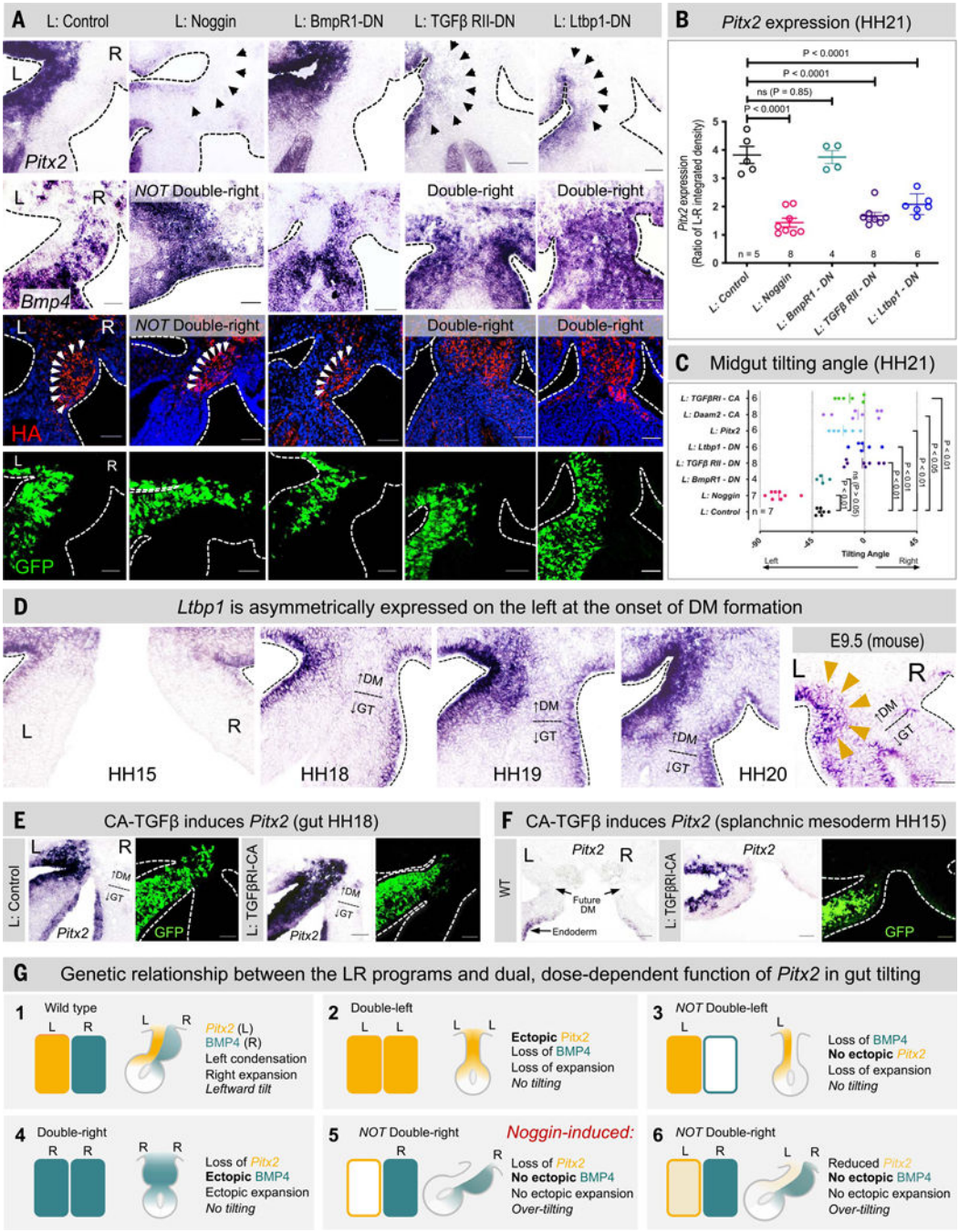

Fig. 4. Latent TGFβ directs gut-specific asymmetry through *Pitx2* expression.

(**A**) *Pitx2* and *Bmp4* expression (ISH), HA (red), and gut tilting upon specified electroporations in the chicken DM cells marked by GFP. (**B** and **C**) *Pitx2* expression (B) was compared with one-way ANOVA followed by multiple comparisons with Tukey's correction (presented as mean ± SEM), and gut tilting (C) was compared using Watson's test (presented as a circular mean). (**D**) *Ltbp1* in chicken and mouse DM (ISH). (**E** and **F**) TGFβ RI-CA electroporation in chicken DM cells marked by GFP (E) drives *Pitx2* expression in the gut and splanchnic mesoderm (F). (**G**) *Pitx2* specifies the left side by suppressing *Bmp4*

(**1** to **4**); *Pitx2* also directs gut-tilting morphogenesis, a function of *Pitx2* unmasked only in the absence of the double-right phenotype (**4** to **6**). Scale bars, 50 μm.

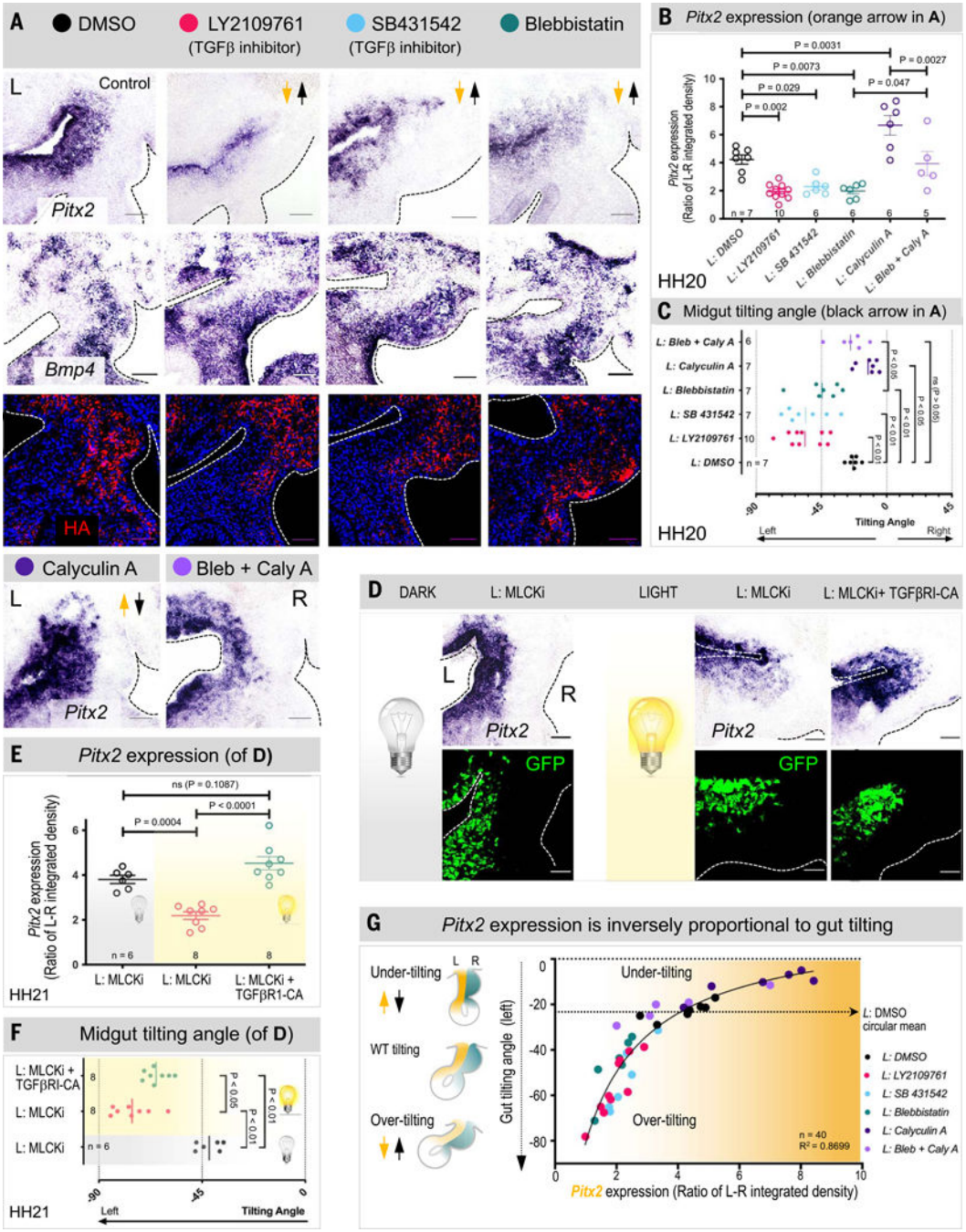

Fig. 5. The contractile status of the DM is mechanically sensed by TGFβ-*Pitx2*.

(**A**) *Pitx2* and *Bmp4* expression (ISH) and HA (red) upon resin beads coated with specified drugs. (**B** and **C**) *Pitx2* expression (B) was compared with one-way ANOVA, followed by multiple comparisons with Tukey's correction (presented as mean ± SEM), and gut tilting (C) was compared using Watson's test (presented as circular mean). (**D** to **F**) *Pitx2* expression [quantified in (E)] and gut tilting [quantified in (F)] upon electroporating photoactivatable myosin light chain kinase (MLCK) or MLCK/TGFβ RI-CA in chicken DM

cells marked by GFP. (**G**) Negative correlation between *Pitx2* expression and gut tilting, fitting a nonlinear regression curve (R^2 = 0.8699, HH20). Scale bars, 50 μm.

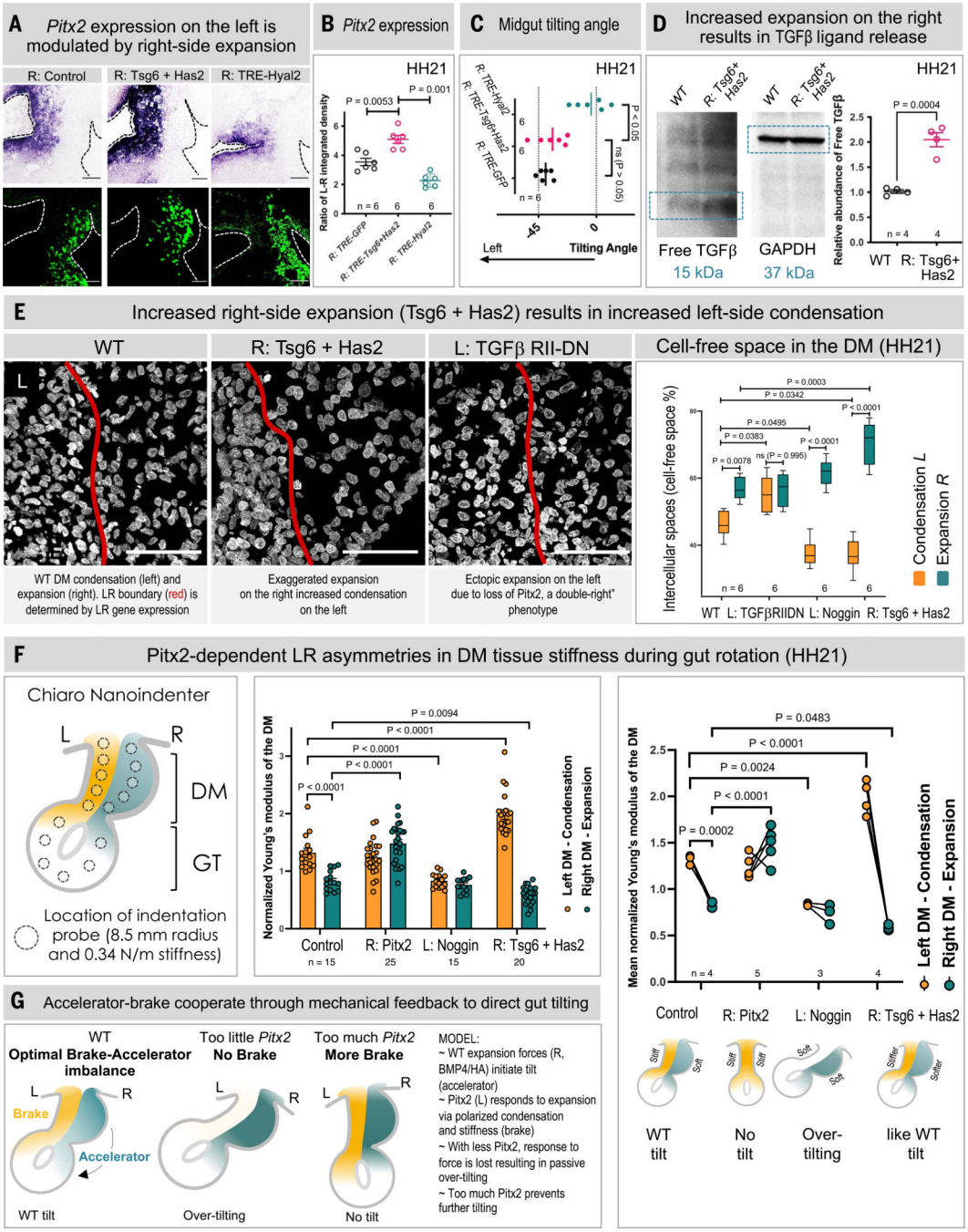

Fig. 6. *Pitx2* patterns DM stiffness on the left by mechanical feedback with the right.

(**A**) *Pitx2* expression (ISH) and gut tilting upon loss of expansion (Hyal2) or exaggerated expansion (*Tsg6* plus *Has2*). (**B** and **C**) *Pitx2* expression (B) was compared with one-way ANOVA followed by multiple comparisons with Tukey's correction (presented as mean ± SEM), and gut tilting (C) was compared using Watson's test (presented as circular mean). (**D**) Exaggerated expansion increased free TGFβ on Western blot with control GAPDH and densitometric quantification by unpaired *t* test (presented as mean ± SEM). (**E**) DM mesenchymal cell compaction measured by percentage of internuclear space (DAPI) in

wild-type and electroporated left and right sides of the chicken DM. Statistics were analyzed by one-way ANOVA followed by multiple comparisons with Tukey's correction (presented as mean ± SEM). (**F**) Indentation measures chicken DM stiffness (HH21). Quantifications were obtained by analyzing independent measurements (graph on the left) or by biological replicates (right) and normalized to the average stiffness of the gut tube. Statistics for left versus right comparison for conditions were analyzed by unpaired *t* test and across conditions by one-way ANOVA followed by multiple comparisons with Tukey's correction (presented as mean ± SEM). (**G**) Model for accelerator-brake mechanical feedback to rotate the gut. Scale bars, 50 μm.

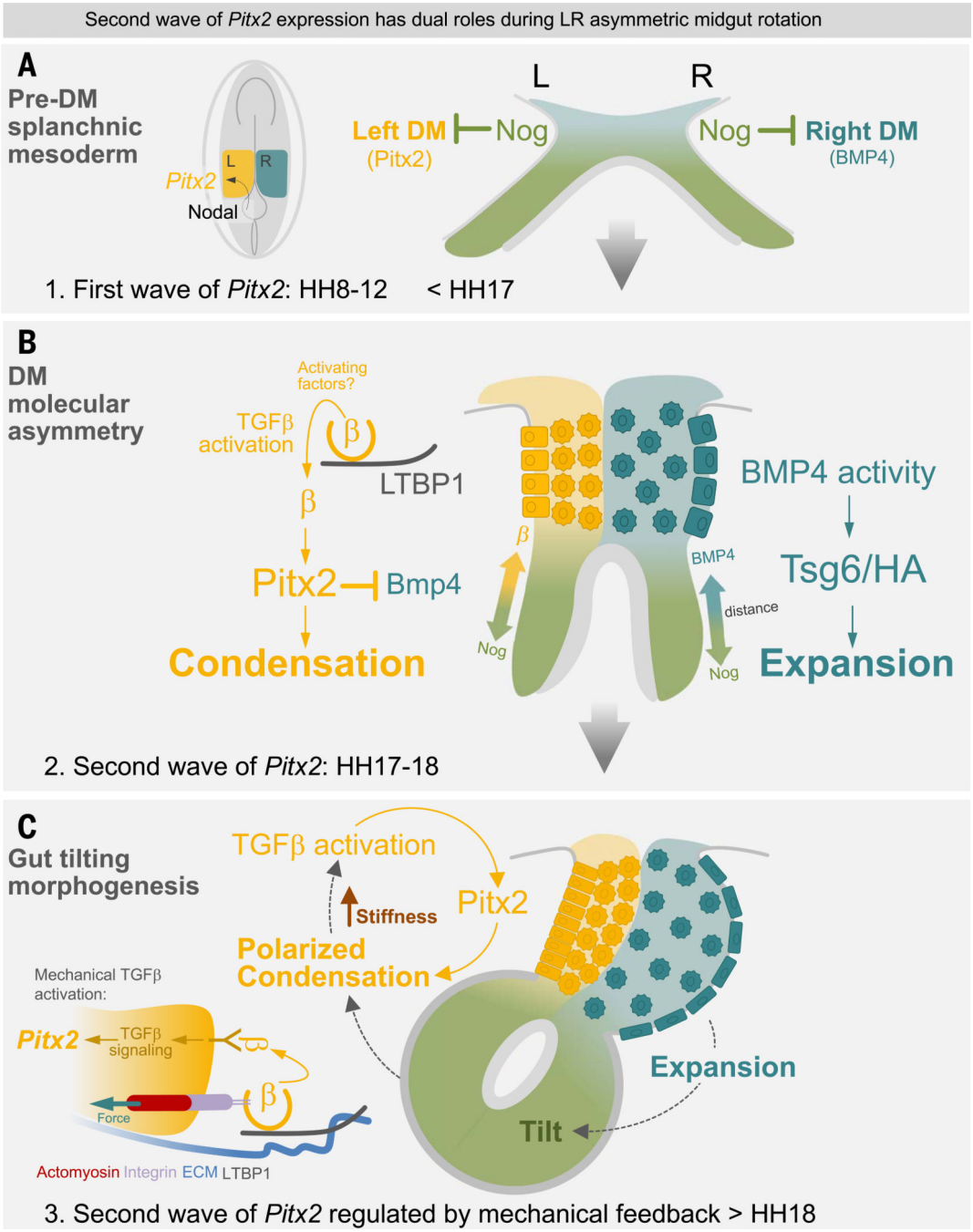

Fig. 7. Second wave of *Pitx2* expression has dual roles during gut rotation.

(**A**) *Pitx2* expression is first initiated by *Nodal* at the node (first wave, HH8) but diminishes in the splanchnic mesoderm after HH12. Noggin in the splanchnic mesoderm ensures TGFβ and BMP signals are sequestered, preventing premature development of asymmetric LR programs. (**B**) First role of *Pitx2* to establish DM left-side identity: As the DM forms (HH17), the Noggin-rich gut tube primordium shifts ventrally, and the second wave of *Pitx2* expression appears, enabling the initiation of DM asymmetries. Regulated downstream of TGFβ, *Pitx2* expression on the left represses *Bmp4* to specify the DM left side. Confined to

the right, BMP4 activity drives Tsg6/HA-mediated ECM expansion to initiate the leftward tilt (HH18). (**C**) Second role of *Pitx2* regulating gut-tilting morphogenesis. Tilting forces from expansion on the right (accelerator) potentiate TGFβ activation on the left (>HH18). The consequential *Pitx2* accumulation induced by TGFβ inhibits gut tilting through polarized mesenchymal cell condensation and tissue stiffness. Inset on the left depicts the release of free TGFβ cytokine from the latent complex. TGFβ pro-peptide (orange open circle) is bound to LTBP1 (gray). Cytoskeletal contraction forces (red, actomyosin filaments) engage integrins (purple) to release active TGFβ free to bind its receptor and activate TGFβ signaling.